

Experimental Study of a TLP Offshore Floating Wind Turbine

Elif Oguz^{1*}, Alexander H. Day¹, David Clelland¹, Atilla Incecik¹, Saishuai Dai¹,

Juan Amate Lopez², Gonzalo González², Gustavo D. Sánchez²

1. Naval Architecture, Ocean and Marine Engineering Department, University of Strathclyde, Glasgow G4 0LZ, UK

2. Iberdrola Ingeniería y Construcción, Madrid 28050, Spain

Abstract: Tank testing in a wind and wave environment is a key part of the design process for the development of an offshore floating wind turbine. The current paper describes an extensive experiment campaign carried out at the Kelvin Hydrodynamics Laboratory at the University of Strathclyde to determine the hydrodynamic performance of the Iberdrola TLPWIND offshore floating wind turbine with the NREL 5MW reference turbine over a range of environmental conditions. Tests were carried out for 70m water depth and the deployment area selected as off Aberdeen, North Sea. The campaign included free oscillation tests, tests in regular waves and irregular waves, and additionally examined failure and accidental load cases.

Keywords: renewable energy; offshore floating wind turbines; TLPWIND[®]; testing; tension leg platform

Article ID: 1671-9433(2010)01-H109-00

1 Introduction

In the recent years, interest in wind energy has shifted towards floating offshore wind turbines (FOWTs). Today, different attempts are made in many international projects to create alternative floating offshore platforms, where installation of wind turbines also plays an important role.

One of the most important aspects in harvesting offshore wind energy is water depth. When the water depth is more than 50m, fixed foundations become an expensive and challenging solution. Consequently many researchers are currently focusing on the application of FOWTs in intermediate and shallow water. The tension leg platform wind turbine (TLPWT) has been selected by IBERDROLA in order to contribute to alternative floating offshore wind turbines in moderate water depth.

The TLP wind turbine has recently attracted interest as a system for moderate water depth, due to the reduced heave, pitch and roll motions compared to other floating platforms and the potential to offer significantly reduced structural costs due to the reduced steel weight.

In the UK there are a number of sites in the North Sea which are in the range of water depth from 50-100m. This paper summarises an extensive experiment campaign to investigate the performance of a TLP wind turbine suitable for deployment in a UK site. The tests were carried out by the University of Strathclyde in cooperation with IBERDROLA under the framework of the TLPWIND UK research and development project funded by InnovateUK.

2 Experimental Setup

The model tests were carried out in the Kelvin Hydrodynamics Laboratory at the University of Strathclyde. The tank has dimensions of 76 m L x 4.6 m W x 2.5 m D, and is equipped with a four-paddle absorbing wavemaker, capable of moving vertically to accommodate water depths from 1.6m to 2.3m which can generate both regular and irregular waves over 0.6m in height. An extended beach of 12m length was constructed to improve the absorption over the frequency range of interest. Reflection coefficients less than 5% were observed over a frequency range from 0.3-1.2Hz.

Tests were aimed at determining the response of the TLPWIND offshore floating wind turbine. The geometry and all mass properties of the floater and turbine were modelled using Froude scaling. The model is shown in Fig.1.

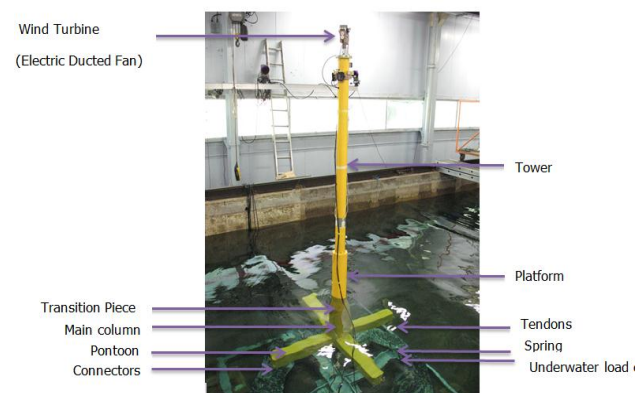


Fig.1 Experimental setup

3 Instrumentation

The instrumentation package installed on the model is shown in Fig. 2 and summarised in Table 1. The water surface profile was measured via 2 wave probes; one located 10m from the

Received date:

Foundation item: Supported by Innovate UK

*Corresponding author Email: e.oguz@strath.ac.uk

face of the wave maker (tank wave) and one in-line with the model (model wave). The six-degree-of-freedom floating body motions were measured using a Qualisys optical tracking camera system. Strain gauges were installed to measure tower bending moments. Turbine thrust was measured using a load cell located at the base of the fan. Tendon tensions were measured at the bottom of the tank using 8 underwater load cells. A 3 axis accelerometer was mounted at the model VCG and a second 3 axis accelerometer mounted at the top of the tower to obtain the accelerations at COG and at tower.

A range of different approaches have been used in previous studies to simulate the wind loading on floating wind turbines in the laboratory environment. In the present study, a “software in the loop”(SIL) method developed by CENER has been deployed to generate the aerodynamic thrust loads (see Day et al. (2015)). This approach does not require the generation of wind over the tank or the construction of a working scaled rotor.

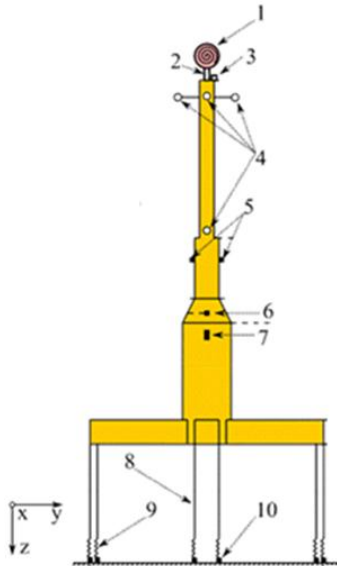


Fig. 2 Instrumentation Package

Table 1: Instrumentation summary

ID	Contents	Measurement
1	Electric Ducted Fan (EDF)	
2	Beam Load Cell (measure thrust)	Fan Thrust
3	Wireless accelerometer	Acceleration at nacelle
4	Qualisys motion capture reflection markers	6 DOF motion of platform
5	Strain gauges	Tower bending moments
6	Wired accelerometer at VCG (inside)	Acceleration at CG
7	Water proof camera (inside)	
8	Tendon wires (8 in total)	
9	Springs (8 in total)	
10	Under water load cell (8 in total)	Tendon tension

Using the six degree of platform motions measured during the tests, the aerodynamic thrust related to the instantaneous position and velocity of the platform are calculated in real time using a modified version of the FAST aero-hydro-servo-elastic software code. The calculated values for scaled thrust load are used to drive a calibrated high-speed fan (Electric Ducted Fan, EDF) located on the model in line with the rotor drivetrain to generate the thrust component of the wind load.

4 Model Installation

The model was installed at the midpoint of the tank (Figure 1) on a mounting frame installed on the base of the tank arranged to allow the model to be rotated through 45 degrees. A detailed drawing of the plan and profile view of the tank showing the experimental setup is given in Fig.3.

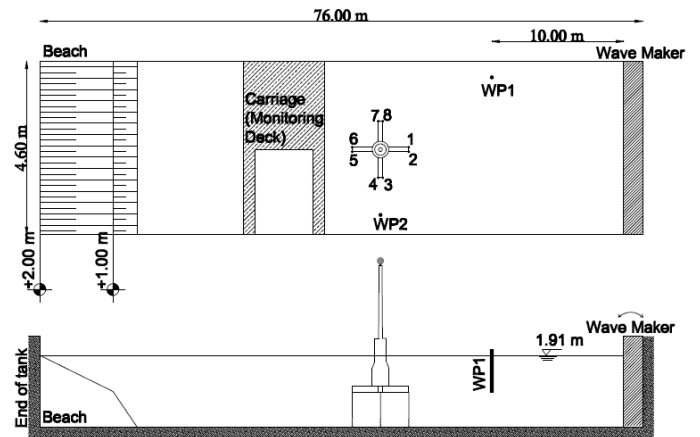


Fig.3 Schematic view of the model installed in the tank

Apart from a set of tests conducted to define the effect of varying water depth on the system due to tide, the water depth was kept at a value of 70m in full scale for all tests.

Since tendon performance is critical to the performance of a TLP, great care was taken to ensure that pretension and stiffness were correctly adjusted. The eight tendons were constructed using stainless steel wires, and the full-scale tendon stiffness was modelled using calibrated springs. The tendons were attached at both ends to universal joints to minimize friction. The model was designed to allow the tendon tension to be adjusted from above with the model at the correct draft and the water level at the design value. Since the weight of the tendons could not be correctly scaled, appropriate corrections were made to the expected value of the pre-tension to allow the model to be installed correctly.

After a process of careful adjustment, the mean tendon tension was less than 3% of the target value.

5 Free Oscillation Tests

Six sets of free oscillation tests were carried out to characterise the damping coefficients and natural periods of the system in four different modes of motion as described in Table 2. Each test was repeated at least ten times. The surge tests were carried out for three conditions to understand the

importance of the wind effect on the system damping: no wind, constant predefined thrust (PT), and software in the loop (SIL) controlled thrust, with wind speeds corresponding to the rated wind speed for the turbine.

The tests were carried out by displacing the structure in the mode of motion and carefully releasing it. In the case of heave and pitch it proved extremely difficult to achieve reliable results due to the high stiffness of the system, the difficulty of imposing sufficient motion without exciting other modes, and the rapid decay. Consistent results were achieved in surge and yaw.

Table 2: Free Oscillation Tests

Test ID	Contents
D1001	Surge (no wind)
D1002	Surge (PT $w_s=11.4\text{m/s}$)
D1003	Surge (SIL $w_s=11.4\text{m/s}$)
D1004	Yaw (no wind)
D1005	Heave (no wind)
D1006	Pitch (no wind)

It was relatively easy to displace the structure in surge without inducing other motions. Sample results for surge are shown in Figure 4. This shows the offset generated by the mean wind. It can be seen that the wind has almost no impact on the natural period, with the mean period for the SIL case found to be around 1% lower than with no wind.

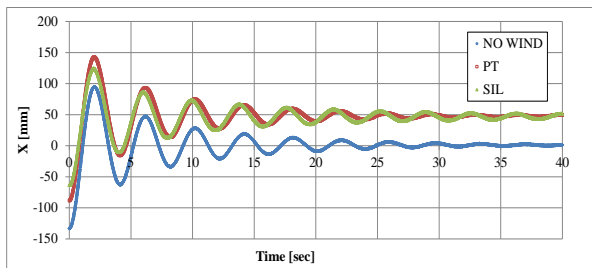


Figure 4 Free Oscillation Tests in surge

The data was analyzed by fitting an analytical solution for a linear spring-mass-damper system to the time history:

$$x(t) = \bar{x} + \hat{x} \exp(-\zeta \omega t) \cos\left(\left(1 - \zeta^2\right) \omega t - \phi\right)$$

The linear model yielded a good fit for surge in no wind, as shown in Figure 5. The quality of fit was similar for the constant predefined thrust; however with SIL active, the damping exhibited a more strongly non-linear response, and the fit for the SIL case improved noticeably once a combination of linear and quadratic damping was employed.

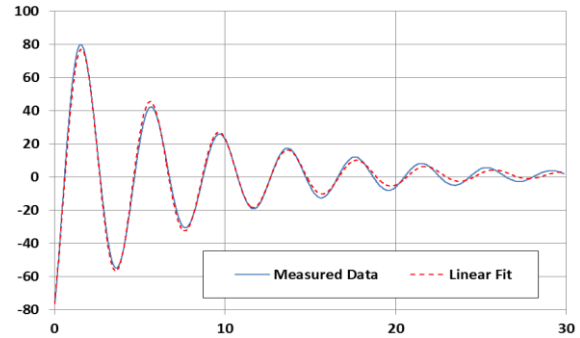


Figure 5 Typical fit for surge (no wind)

6 Regular Wave Tests (RAOs)

Regular wave tests have been carried out to characterize the behavior of the structure through the motion RAOs and transfer functions for tendon tensions, tower bending moments, and accelerations. Four sets of tests were performed. Three sets in head seas following the pattern of the tests described above used no wind, constant predefined thrust, and SIL respectively. Tests were performed in regular waves with a target amplitude of 1.0m at full scale. Tests with wind used a full-scale wind speed of 11.4m/s, the rated speed of the NREL 5MW turbine. Wave frequencies varied from 0.25-1.0 Hz at model scale, corresponding to full scale periods in the range 6-30 s.

A typical set of data for motions is shown in Fig.6. In this figure, the signals are in the following order from top: Wave / Pitch / Yaw / Z / Y / X, where X is the longitudinal displacement, Y is the transverse displacement, and Z is vertical displacement. In each case the green trace is the recorded data and the red trace is a sinusoidal fit. The wave elevation from the model tests fitted extremely well to the sinusoidal form, as expected. In some cases the response data presented could also be based on the amplitudes of sinusoidal functions fitted to the experiment data using a similar non-linear least-squares fitting procedure, and with frequency essentially identical to the waves; this can be seen for the longitudinal motion in Figure 8.

However, in some cases the response is far from sinusoidal, even though the period of the response is equal to the wave period. In Fig.6, for example, it can be seen that the (very small) yaw response resembles a saw-tooth wave. In some other cases the response is at some harmonic of the wave period. For example the vertical motion in Fig.6 exhibits a frequency double that of the planar motions, and furthermore the response is clearly non-sinusoidal, with amplitude of successive minima alternating in amplitude. Hence responses were typically characterized in terms of the range of response rather than the amplitude of a fitted sinusoid.

The surge and heave motion responses for the case of head waves and no wind are presented in Figure 7. Note the widely varying magnitude of the responses: heave motions are an order of magnitude smaller than surge motions.



Fig.6 Typical recorded wave and motion data (head waves no wind) From top: Wave / Pitch / Yaw / Z / Y / X

As expected, the peak of the surge RAO occurs at a frequency equal to that found in the free oscillation tests. Heave is coupled to surge through the kinematics of the tendons, and hence it is expected that the frequency of peak heave corresponds to the peak surge. Heave response is at twice the frequency of the planar motions, as shown previously in Fig.6. The highest vertical displacement occurs with the tendons upright, and the platform is displaced downwards as it surges both forward and backwards relative to the wave direction. The magnitude of the cycles alternate due to a slight mean offset of the platform in surge.

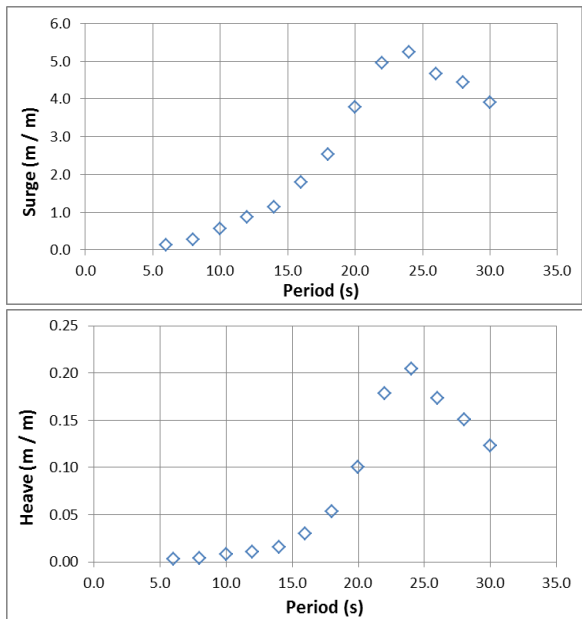


Figure 7 RAOs for Surge and Heave motions of Floater: Head waves, No Wind

As the wind is deployed this mean offset of the platform increases, and the damping changes somewhat; these effects naturally have some impact on the motions. In particular, the heave motion changes. The difference in magnitude between alternate cycles increases, as shown in Figure 8; as the mean offset increases, the platform displacement is greater in the downwind direction than in the upwind direction, and hence the asymmetry between the cycles is magnified. As the wind speed increases, the mean offset increases, and it could be expected that once the mean offset is greater than the surge

amplitude, the platform would respond in heave at the wave frequency rather than at double the wave frequency.

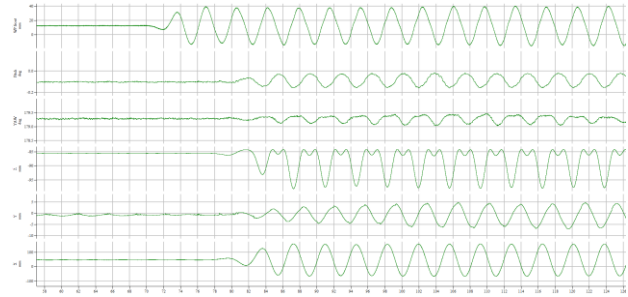


Figure 8 Typical recorded wave and motion data (head waves + SIL) From top: Wave / Pitch / Yaw / Z / Y / X

The largest response naturally is in the surge direction, and hence it is interesting to examine what impact the simulated wind has upon the surge RAO. The comparison is shown in Figure 10. It can be seen that the response for the case with no wind is larger than that with the wind simulated using SIL. This is as might reasonably be expected, since it is known that the aerodynamic forces contribute to the damping of the structure motion. The RMS difference in RAO is 9%, the largest difference is around 20% at a full-scale period of 20s, and the difference at the peak of the RAO is about 6%.

In a similar manner it is interesting to compare the motions in the wave direction in the case of quartering seas with those for head seas. This is shown in Figure 10 for the case with no wind. It can be seen that the platform motion is relatively insensitive to the wave heading.

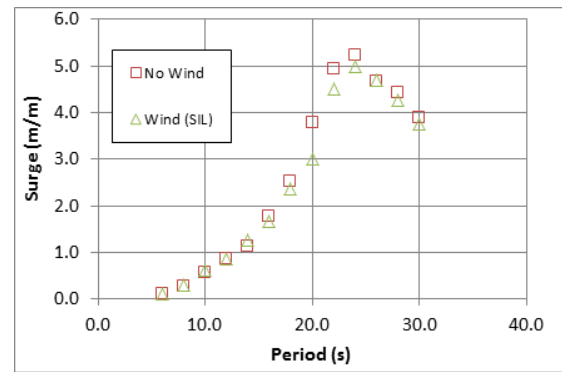


Figure 9 Surge RAOs with and without wind

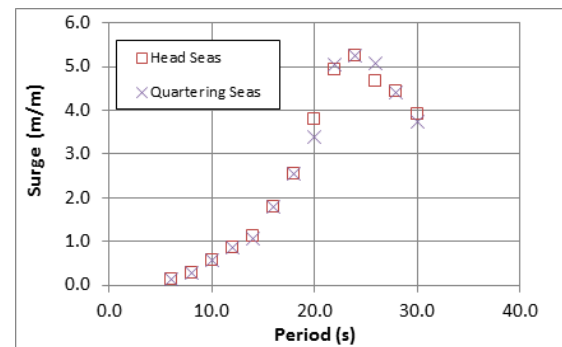


Figure 10 Longitudinal motion RAOs for two different wave headings

7 Tests in Irregular Waves

A series of irregular wave tests were conducted to characterise the platform response in a realistic sea environment. 8 different sea states with different wave and wind conditions were used (Table 3). All sea states were generated for a period corresponding to three hours at full scale. Variations in wind direction were accommodated by rotating the fan on top of the tower.

All sea states were calibrated before the structure was deployed using measurements taken at the still-water position of the TLP. Significant wave heights were adjusted to be correct to within 2% of target values in all cases.

Table 3: Sea States

Sea State	Hs (m)	Tp (s)	Wind Speed(m/s)
N1	4.55	9.00	11.40
N2	1.50	6.61	11.40
N3	8.46	10.13	38.76
N4	0.75	5.44	6.05
N5	1.25	6.36	9.18
N6	1.75	6.86	12.80
N7	2.75	7.80	16.80
N8	6.00	10.28	25.00



Figure 11 Example of Irregular Wave Test

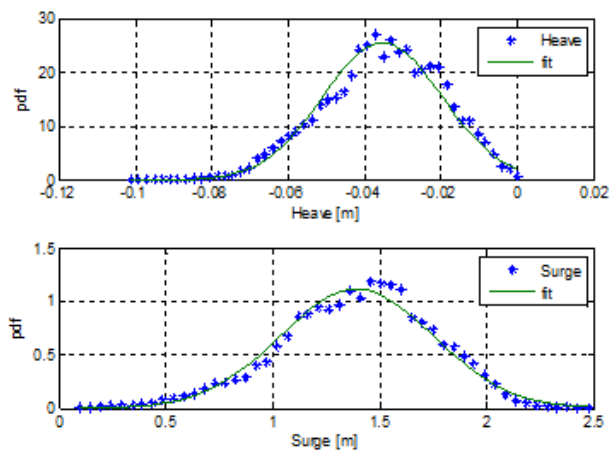


Figure 12 Probability Density Functions for Heave and Surge

A total of 53 cases were tested. Results were computed in terms of probability density functions of the various parameters. Sample results for full scale PDFs for surge and heave are shown in Figure 12, along with the best fit Gaussian distribution.

8 Special Tests

In addition to the conventional tests described previously, a series of special test cases were investigated. These tests are explained briefly in the following section.

8.1 Variable Water Depths

In order to investigate the effect of varying water depth due to tide; two water depths (LAT- lowest astronomical tide- and HAT- highest astronomical tide- levels) were tested for two different sea states, two different wave headings (0 and 45 degree) and four different wind headings (0, 180, 225 and -45 degree). The LAT level was set at 68.36m water depth and the HAT level set at 74.90m. All measured tendon tensions and platform motions have been analyzed for these two water depths.

8.2 Emergency Stop Tests

The main aim of these tests was to determine the impact on the TLP of a sudden turbine stop. This is carried out using the SIL system which is programmed to stop the fan suddenly. A typical time history of the key variables is shown in Figure 13. The first signal is the wavemaker trigger. This is used to synchronize the points at which the wavemaker starts, and at which the turbine stops, to allow investigation of the sensitivity of the results to exact point on points on the wave cycle. The second signal is the wave probe in line with the model; the third signal is the surge displacement of the model, while the final signal is the thrust generated by the fan. It can be seen that the model takes up a steady offset in surge before the waves arrive, and then when the fan stops and the thrust drops to zero, the platform exhibits a response similar to that of a free oscillation test in the presence of waves.

In total, 44 cases for emergency stop condition were carried out.

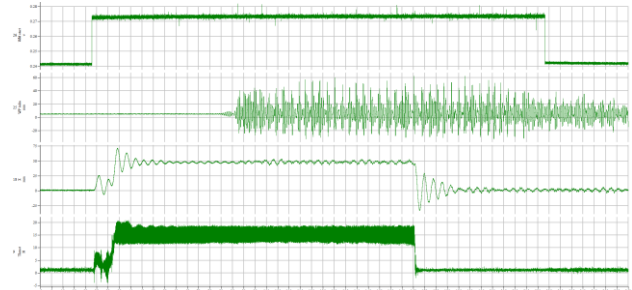


Figure 13 Typical recorded data for emergency stop tests

8.3 Tendon Loss Tests

The final set of special cases examined the behavior of the TLPWIND UK platform when one or more tendons had failed. These tests were designed to determine the margin for

safety in the remaining tendons. Three different failure modes were analysed, with tendons numbered as shown in Figure 14: First loss of tendon 1, loss of tendon 3 and finally loss of both tendons.

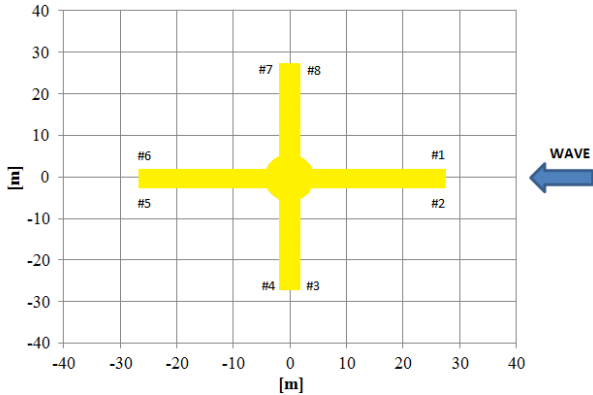


Figure 14 Tendon numbering

9 Installation Tests

In addition to the tests on the floater, a further series of tests were carried out on the installation vessel designed for this platform. The vessel consists of a customised semi-submersible barge to which the floater is attached during the tow out operation. Once at station the barge is ballasted to the connection draft; the tendons are connected, and the barge de-ballasted and towed back to port.

These tests were carried out at a smaller scale due to the size of the barge. Tests consisted of towing tests at tow out and return conditions, sea-keeping tests we are carried out at four different drafts representing the installation process. The barge and floater at connection draft are shown in Figure 15.

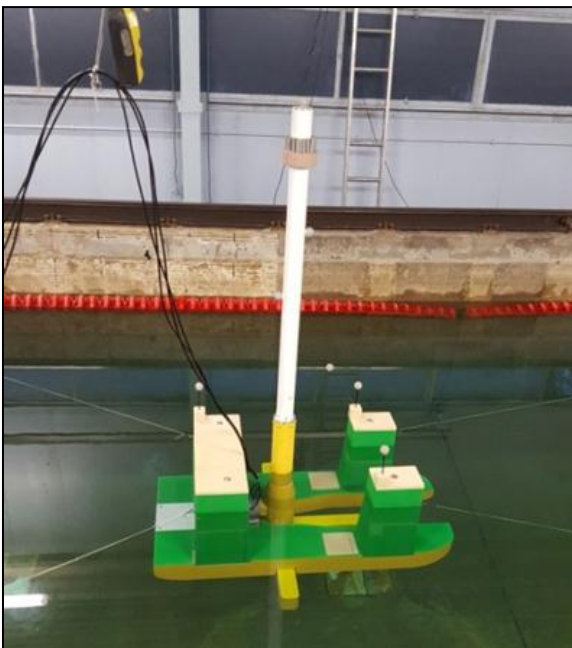


Figure 15 Installation barge at connection draft

A sample set of results for the final connection draft are shown in Figure 16 for wave heading= 0°, $H_s= 2.75m$, $T_p=7.8s$.

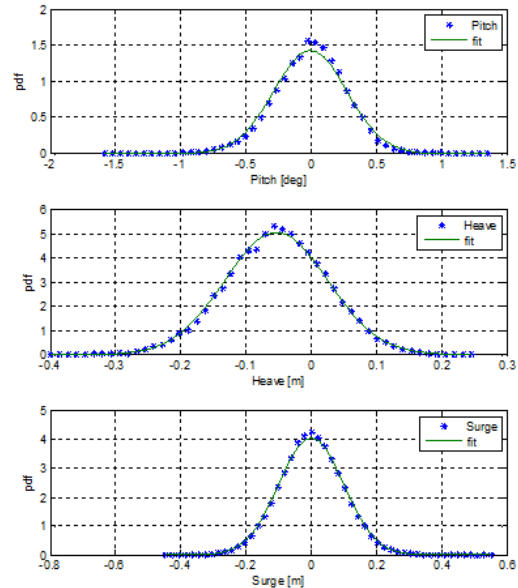


Figure 16 Probability density functions for Pitch, Heave and Surge motions

10 Conclusion

An extensive campaign of experiments were carried out under the framework of the “TLPWIND UK” project to characterize the hydrodynamic performance of a 70m water depth TLP offshore wind turbine system. In this paper, the experimental setup, free oscillation tests, motion RAOs, irregular wave tests and installation tests have been described.

Acknowledgement

The work was funded under the InnovateUK grant “TLPWind UK: Driving down the cost of offshore wind in UK waters”, project reference 101969. The authors acknowledge the support of Iberdrola and CENER to this work.

References

Day AH, Babarit A, Fontaine A, He YP, Kraskowski M, Murai M, Penesis I, Salvatore F, Shin HK (2015). Hydrodynamic modelling of marine renewable energy devices: A state of the art review. *Ocean Engineering*, **108**, 46-69.

Zamora Rodriguez R, Gomez Alonso P, Amate Lopez J, De Diego Martin V, Dinoi P & Souto Iglesias A (2014). Model Scale Analysis of a TLP Floating Offshore Wind Turbine. *OMAE 33rd International Conference on Ocean, Offshore and Arctic Engineering*, San Francisco, California, USA